Classification of Polyethylene Particles and the Local CD3+ Lymphocytosis
in Histological Slice Images

Lara-Maria Steffes[1], Marc Aubreville[1], Stefan Sesselmann[2], Veit Krenn[3], Andreas Maier[1]

[1]Pattern Recognition Lab, Computer Sciences, Friedrich-Alexander-Universtität Erlangen-Nürnberg, Germany
[2]Professor for Innovative Concepts and Technologies in Healthcare, OTH Amberg-Weiden, Germany
[3]Center for Histopathology and Molecular Pathology, Trier, Germany
Lara.Steffes@gmx.de

Abstract. In 2014, about 400.000 endoprosthetic operations were performed in Germany [1]. Unfortunately, the lifespan is limited and already after 10 years 5 percent of the patients have primary complaints [2]. All the more important it is to clarify the causes for this failure. One main cause is an immune response to abrasion particles of the implant, an effect which is assumed to be correlated with occurrence and count of CD3+ immune/inflammatory cells [3]. For the further analysis of this effect, computer-aided classification and image analysis methods provide a high value for the medical research. Aim of this work was the development of an threshold-based algorithm for the segmentation of polyethylene abrasion particles and the CD3+ immune/inflammatory response of histological slice images.

1 Introduction

In Germany, arthroplasty, especially hip and knee endoprosthesis, is one of the most often performed surgical procedures. In 2014, about 400.000 endoprothetic operations were done [1]. For the patient, artificial endoprosthesis offers a large gain in quality of life, as pain is reduced and lost mobility is restored. Often, sporting activities can be exercised again. Unfortunately, the lifespan of endoprotheses is limited. Already after 10 years, approximately 5 percent of the patients have primary complaints, i.e. they are no longer without pain [2]. The cause of failure of endoprosthesis can be multifactorial. The main unsolved problem is the loosening of the implant from the bone and the formation of a synovial-like interface membrane (SLIM) between the implant and the bone [2]. Different abrasion materials, dependent on the used material of the sliding pair of the endoprothesis, can be found in the SLIM and are discussed to have an influence on the loosening process [3]. The occurrence and count of CD3+ immune cells, which play a central role in the immune defense, is thought of as

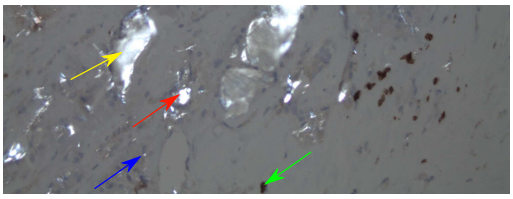

Fig. 1. Histological image with SMPE (yellow arrow), MacroPE (red arrow), MPE (blue arrow), and CD3+ immune/inflammatory response (green arrow).

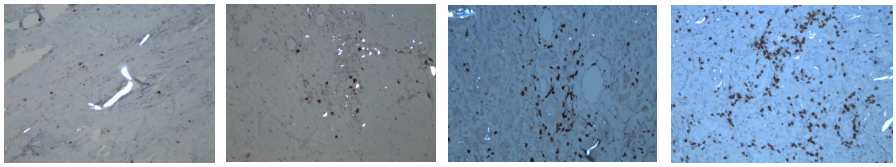

Fig. 2. Different histopathological images with a high variation in color and brightness.

being correlated with this deterioration process. In Fig. 1 the different forms of the polyethylene (PE) particles and the CD3+ immune/inflammatory response are shown. Micropolyethylene (MPE) particles have an expected size of less than 5 μm, macropolyethylene (MacroPE) particles between 5 μm and 100 μm and supramacropolyethylene (SMPE) particles above 100 μm [4]. Because of a high time effort to count every abrasion particle (AP) and the local CD3+ immune/inflammatory response manually and the associated error susceptibility, the aim of this work is the segmentation and classification of the polyethylene APs of different sizes, and the local CD3+ immune/inflammatory response with a semi-automatic threshold-based algorithm.

2 Materials and Methods

For this work, 100 labeled images of stained specimen, collected from 52 patients, were available. The 100 RGB images had a fixed width of 594 μm, corresponding to 2048 pixels. For all images the strength of the CD3+ immune/inflammatory response, the number of MacroPE/SMPE particles and the class of the MPE particles were available as reference. They were labeled semi-quantitatively by a medical expert. To avoid an optimization on the test data set the images were separated into three groups: 60 images for classifier training, while in each case 20 images were used for validation and evaluation. Two different kinds of methods, preprocessing and classification methods, were used for this work. In the preprocessing step the images were first normalized, because of color and intensity variations (see Fig. 2). In literature, different approaches for the standard H&E staining of medical histological images can be found. Coloring with hematoxylin accounts for a blue-purple hue and tissue colored by eosin are visible in a bright pink color [5,6]. The images received for this work were not colored with

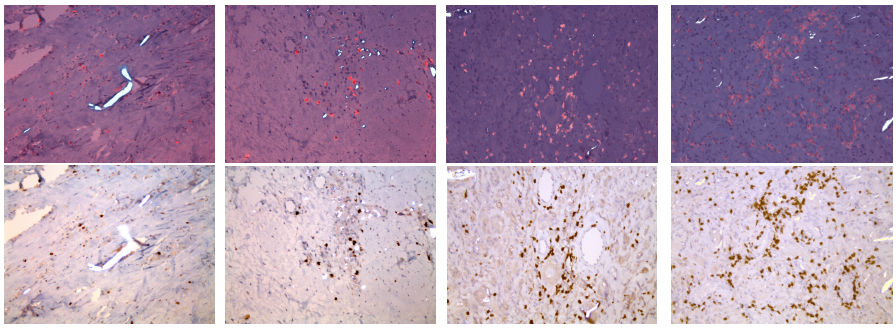

Fig. 3. Top: Macenko normalized histopatological images; Bottom: Reinhard normalized histopatological images.

the usual H&E staining, because eosin would lead to a worsening of the recognition of the CD3+ cells. Nevertheless, two normalization algorithms, Macenko [7] and Reinhard [8] normalization, which were successfully used for H&E stained images, were evaluated and yielded good results (see Fig. 3). Macenko et al. uses a linear per-channel normalization in optical density space [7,9]. Reinhard et al. maps the standard deviations and means of the three channels of the original image to the corresponding channels of the target image in LAB color space [8,9]. Both normalization algorithms are part of the stain normalization toolbox from the University of Warwick [9]. With the help of a color deconvolution (CD) [6] into the three channels corresponding to the actual stain color the visibility of the CD3+ cells and, in the most cases, the PE particles could be improved. With further preprocessing methods, simple binary thresholding, morphological operations for removing small black holes within and cracks in-between larger PE particles and a median filter for noise reduction, binary images were obtained. The PE particles, respectively the CD3+ cells, were visible as white regions on a black background. With a final blob detection method, based on the difference of Gaussian [10] and the assumption of a circular structure of the CD3+ cells, the features of the CD3+ cells were obtained. As output, the number of blobs, the area, the radii and midpoints of the blobs in the image were returned. For the purpose of classification the CD3+ immune/inflammatory response the absolute number and the total area share of these cells per image, were suitable. For finding the features of the PE particles, the number of PE particles, the areas, the perimeters and the contours, a simple contour finding algorithm provided by the OpenCV library was used. As features for separating the PE particles into MPE and MacroPE/SMPE, the perimeters and the total area occupied by PE particles per image were chosen. For classifying the MPE particles, it turned out that the number and the area of MPE particles per image were suitable. For classification the three supervised classifiers Naive Bayes (NB), support vector machine (SVM) and random forest (RF) were used.

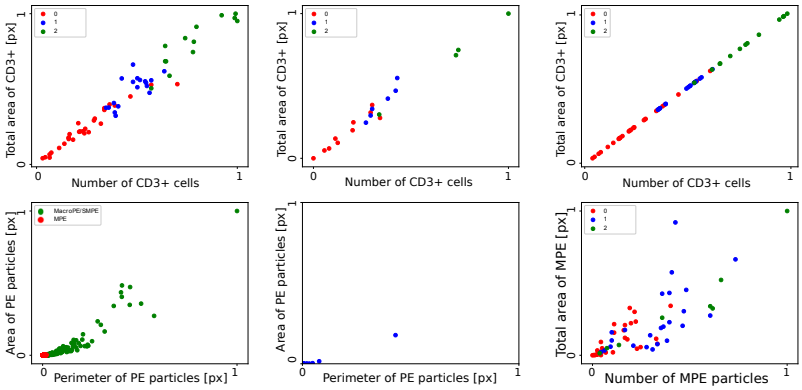

Fig. 4. Top: Ground truth labels (color coded) and CD3+-related features (number of cells, total area of cells). Left: Training set, middle: Test set, right: Training set after PCA; Bottom: PE-related features (perimeter of PE particles, area of PE particles) and MPE-related features (number of MPE particles, total area of MPE particles). Left: PE training set, middle: PE data set of a single test image, right: MPE training set.

3 Results

MPE particles were separated into low, moderate and high. CD3+ cells were separated into low, moderate and high immune/inflammatory response and PE particles have to be divided into MPE and MacroPE/SMPE. In Fig. 4, the normalized numbers and areas of CD3+ cells for the 60 training images, the 20 images for testing and the results of a principal component analysis (PCA) are shown top from left to right. According to the predetermined ground truth data, the red dots correspond to a low, the blue ones for a moderate and the green dots for a high CD3+ immune/inflammatory response. Although the features of the CD3+ immune/inflammatory response lie more or less on a diagonal and it can be thereby assumed that both features are correlated, a NB classifier yielded good results. An accuracy of 80 % could be reached. A PCA for dimensional reduction as well as considering just one single feature could not improve the accuracy and reached to similar results. An alternative classification algorithm (SVM, RF) yielded no significant changes in outcome, with the RF tending to overfit the training sample (see Fig. 5 top). In Fig. 4, the normalized perimeters and areas of every PE particles of the PE training set (bottom left), the PE feature set of one single test image (bottom middle) and the normalized number and areas of the MPE particles for the MPE training set (bottom right) are shown, too. The NB classifier used for classification of the count of MacroPE/SMPE yielded a 55 % accurate estimation, or 90 % when a tolerated error of 1 count was introduced. For classifying the MPE particles into the three classes (see Fig. 4), a NB classifier yielded sufficient results again, revealing 80 % accuracy. In Fig. 5 the decision boundaries for the training set are shown on the respective test sets

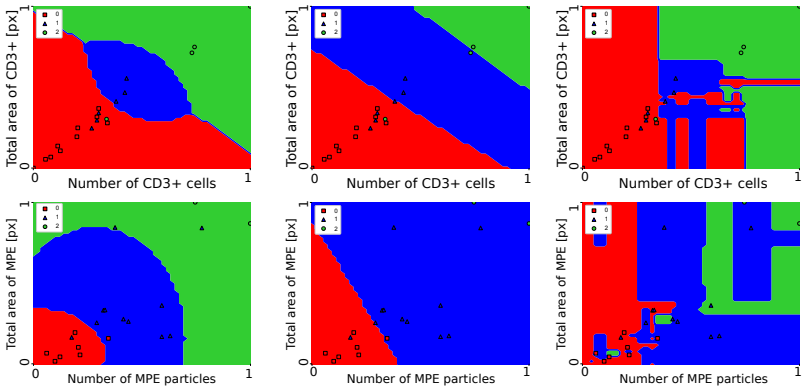

Fig. 5. Top: CD3+ cells decision domains; Bottom: MPE particles decision lines. Left: NB, middle: SVM, right: RF.

truth: \ predicted:	Class 0	Class 1	Class 2
Class 0	10	0	0
Class 1	3	3	0
Class 2	1	0	3

truth: \ predicted:	Class 0	Class 1	Class 2
Class 0	10	0	0
Class 1	4	2	0
Class 2	1	1	2

truth: \ predicted:	Class 0	Class 1	Class 2
Class 0	6	1	0
Class 1	1	8	2
Class 2	0	0	2

truth: \ predicted:	Class 0	Class 1	Class 2
Class 0	6	1	0
Class 1	1	10	0
Class 2	0	2	0

Fig. 6. Confusion matrices. Left: CD3+ classification, right: MPE classification, top: NB; Bottom: SVM.

for CD3+ immune response and MPE classification. In both cases the decision domains are well chosen with NB. In Fig. 6 the different confusion matrices for classifier training are shown.

4 Discussion

Although the popular stain normalization methods are proven and successfully tested for the typically H&E stained colored images, it was possible to apply two of them, Macenko normalization and Reinhard normalization, to histological slice images, which were not colored with the typically H&E staining. Macenko normalization, followed by CD was suitable for the most images to improve the visibility of the available PE particles. Nevertheless sometimes smaller PE particles were not detected anymore. Generally the small image resolution and sometimes even blurred parts seemed to be problematic for the MPE particles detection. This effect accounts for some images of high MPE that were attributed to be of low MPE count and low MPE area by the feature extractor (cf. Fig. 4 bottom right). Using the Reinhard normalization as a preprocessing step provided an effective means of reducing the image colouring variance significantly.

After a further CD it was possible to catch the CD3+ cells with a fix threshold for all images. With the assumption of a circular structure of the CD3+ cells, it was possible to find them, although they were overlapping. Compared to the state of the art, detection of overlapping CD3+ cells was improved noticeably. Generally it can be said, that a higher number of images would have led to a better evaluation and performance of the classifiers. Nevertheless, because of the small set of very meaningful features, a classification of the cells and particles was possible and could convince with good accuracies. Especially, for the medical team it was important to gain a first indication whether the MPE correlates to the CD3+ immune/inflammatory response with a small effort. After this relationship could be confirmed, in a further step a larger study can be created, i.e. with deep learning methods [11], to verify the results and increase precision in detection.

References

1. Liebs TR. EPRD-Jahresbericht 2015. EPRD Endoprothesenregister Deutschland; 2016.
2. Hopf F. Materialabhängige CD3-Response in der SLIM bei dysfunktionalen Gelenkendoprothesen. Freie Universität Berlin; 2016.
3. Hopf F, Thomas P, Sesselmann S, et al. CD3+ lymphocytosis in the peri-implant membrane of 222 loosened joint endoprostheses depends on the tribological pairing. Acta Orthopaedica. 2017; p. 1–7.
4. Krenn V, Hopf F, Thomas P, et al. Supramakropartikuläres Polyethylen bei Entzündungen periprothetischer Membranen. Der Orthopäde. 2016;45(3):256–265.
5. Magee D, Treanor D, Crellin D, et al. Colour normalisation in digital histopathology images. In: Proc Optical Tissue Image analysis in Microscopy, Histopathology and Endoscopy (MICCAI Workshop). vol. 100. Daniel Elson; 2009. .
6. Khan AM, Rajpoot N, Treanor D, Magee D. A nonlinear mapping approach to stain normalization in digital histopathology images using image-specific color deconvolution. IEEE Transactions on Biomedical Engineering. 2014;61(6):1729–1738.
7. Macenko M, Niethammer M, Marron J, et al. A method for normalizing histology slides for quantitative analysis. In: Biomedical Imaging: From Nano to Macro, 2009. ISBI'09. IEEE International Symposium on; 2009. p. 1107–1110.
8. Reinhard E, Adhikhmin M, Gooch B, et al. Color transfer between images. IEEE Computer graphics and applications. 2001;21(5):34–41.
9. Raza SeA. Stain Normalisation Toolbox of Warwick; 2015. [Accessed 2017-09-15]. http://www2.warwick.ac.uk/fac/sci/dcs/research/tia/software/sntoolbox/.
10. Lowe DG. Distinctive image features from scale-invariant keypoints. International journal of computer vision. 2004;60(2):91–110.
11. Aubreville M, Knipfer C, Oetter N, et al. Automatic Classification of Cancerous Tissue in Laserendomicroscopy Images of the Oral Cavity using Deep Learning. Scientific Reports. 2017;7(1):41598–017.